PAPER

Check for updates

Oxygen release/incorporation behavior in hexagonal perovskite BaFeO₃ explored by ^{18}O/^{16}O isotope exchange reactions

Rei Watanabe,[a] Masato Goto, [ID][a] Werner Paulus [ID][b] and Yuichi Shimakawa [ID] *[a]

The 12R-type hexagonal perovskite $BaFeO_3$ containing unusually high-valence Fe^{4+} has a characteristic feature of completely reversible oxygen release and incorporation up to 700 °C in air. Once the structure is established, the unusually high-valence Fe^{4+} state can be stabilized without extreme conditions like a strongly oxidizing atmosphere. During annealing the samples in an $^{18}O_2$ gas atmosphere, almost all oxygen (^{16}O) atoms in the 12R-type $BaFeO_3$ are exchanged with the ^{18}O isotope in an equilibrium process. Thermogravimetric analysis with mass spectrometry in an air-like atmosphere reveals that ^{18}O-exchange-treated 12R-type $BaFeO_3$ releases ^{18}O upon heating and then incorporates ^{16}O on cooling, and the sample reversibly recovers to the initial 12R-type structure. Furthermore, such oxygen release starts at as low as 400 °C, suggesting oxide-ion mobility at such a low temperature. Oxide ions that connect Fe-centered octahedra through both shared corners and shared faces contribute to the oxide ion mobility.

Introduction

Oxygen nonstoichiometry in various transition-metal oxides plays a key role in energy-related applications. For example, oxygen defects and oxide-ion hopping provide mixed ionic and electronic conduction in cathodes of solid oxide fuel cells.[1–3] In oxygen storage materials, oxygen ions are reversibly released and captured from specific crystallographic sites.[4] Transition metal oxides with perovskite or perovskite-related structures are widely studied and practically used for such applications.[5–7] To further improve device performance, achieving appreciable oxide-ion mobility at low operating temperatures is critically important.

Perovskite-structure oxides containing Fe are of particular interest because they show a wide variety of oxygen non-stoichiometry.[8,9] Among them, $BaFeO_3$ polymorphs containing unusually high valence Fe^{4+} tend to easily release oxygen to relieve the instability of the unusual valence state and exhibit contrasting oxygen release and incorporation behaviors.[10] The 3C-type simple perovskite $BaFeO_3$, for instance, starts to release oxygen at very low temperatures, such as at 130 °C, but the oxygen loss in air is irreversible.[10] In contrast, the 12R-type hexagonal perovskite $BaFeO_3$ exhibited a completely reversible change in oxygen content up to 600 °C. Once the 12R-type structure is established, $BaFeO_3$ can reversibly release and

capture oxide ions, even at high temperatures like 600 °C, without extreme conditions like a strongly oxidizing atmosphere.[10]

The 12R-type hexagonal perovskite $BaFeO_3$ contains Fe-centered octahedra that share both corners and faces, as shown in Fig. 1. The fundamental structure is described by a hexagonal cell with the space group $R\bar{3}m$ and the lattice constants of $a \approx 5.8$ Å and $c \approx 28.4$ Å.[11] This framework is a more favorable host for the large Ba^{2+} ions than the cubic 3C structure. In this structure, three FeO_6 octahedra are linked by face-sharing, with a 1:1 ratio of corner-shared and face-shared oxygen sites. The differences in oxygen release and uptake between the 12R-type structure and the 3C-type structure
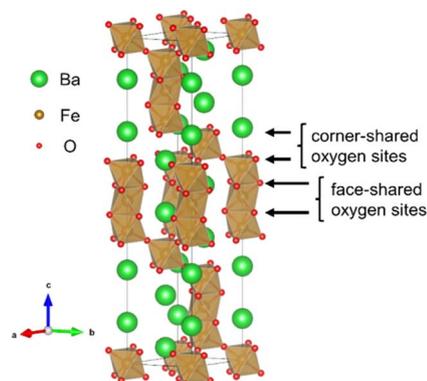
^{a}Institute for Chemical Research, Kyoto University, Gokasho, Uji, Kyoto 611-0011, Japan. E-mail: shimak@scl.kyoto-u.ac.jp

^{b}Institut Charles Gerhardt Montpellier, Université de Montpellier, CNRS, ENSCM, 34000 Montpellier, France

Fig. 1 Schematic structure model of the 12R-type hexagonal perovskite $BaFeO_3$.

suggest that oxygen sites involved in octahedral face-sharing play an important role in the reversible changes in oxygen content. In order to more deeply understand the oxygen non-stoichiometry behavior in the 12R-type $BaFeO_3$, we have substituted ^{18}O for ^{16}O and carried out the thermogravimetric analysis (TGA) of the samples. The oxygen isotope experiment provides insight into the nature of oxide-ion mobility without the need for oxide-ion conductivity measurements.[5,12,13] Considering the natural abundance of oxygen isotopes, 99.76%, 0.04%, and 0.20% respectively for ^{16}O, ^{17}O, and ^{18}O, the $BaFeO_3$ initially synthesized in this study by a normal solid-state reaction consists almost entirely of ^{16}O ions, which are replaced by the heavier ^{18}O isotope by annealing the sample in special $^{18}O_2$ gas. We have confirmed that ^{16}O can be replaced by ^{18}O in the 12R-type hexagonal perovskite structure, suggesting appreciable oxide-ion mobility at temperatures as low as 400 °C. Note that this temperature is much lower than typical operating temperatures of solid-oxide fuel cells and oxygen storage materials.[14,15] With the sample, we discuss two distinct processes related to the oxygen mobility; one involving the loss (incorporation) of oxygen and the other involving the exchange of oxygen while maintaining oxygen stoichiometry. The main process governing the replacement of ^{16}O with ^{18}O is found to depend strongly on the annealing temperature. We also discuss the specific crystallographic sites involved in the oxygen replacement process.

Experimental

The 12R-type $BaFeO_3$ in the present study was prepared in the same manner as reported previously.[11] The oxygen-deficient hexagonal perovskite $BaFeO_{3-\delta}$ ($\delta \approx 0.2$) was first synthesized by heating a mixture of $BaCO_3$ and Fe_2O_3 in flowing $^{16}O_2$. The obtained precursor with the oxidizing agent $KClO_4$ was put into a Pt capsule, and the cell was compressed using a cubic anvil-type high-pressure apparatus through a pyrophyllite medium under quasi-isostatic pressure conditions. After treating the sample at 3 GPa and 1000 °C for 30 minutes, the resulting sample was washed with distilled water to remove residual KCl and $KClO_4$, both of which are water-soluble. Phase identification was carried out by synchrotron X-ray diffraction (SXRD), and the crystal structure of the phase was analyzed by the Rietveld method using the program RIETAN-FP.[16] The crystal structure models were drawn with the program VESTA.[17]

Exchange of oxygen in the 12R-type $BaFeO_3$ samples (each 150 mg) by the ^{18}O isotope was carried out by annealing them in a 70 mL quartz tube filled with 97% $^{18}O_2$ and 3% $^{16}O_2$ gas, a mixture that will hereafter be referred to as $^{18}O_2$ gas. Each of the three samples was treated at 650 °C for 2 days, 400 °C for 4 days, and 400 °C for 6 days, respectively. 650 °C is close to the highest temperature for annealing without causing thermal decomposition. On the other hand, 400 °C is nearly the lowest temperature at which oxygen can be mobile. The amount of ^{18}O exchange in $BaFeO_3$ was estimated by measuring the sample weight change with TGA with mass spectrometry (MS) from room temperature to 700 °C in a 33% O_2/Ar atmosphere, which provides a similar atmosphere to air. The gas contains normal

oxygen with 99.76% ^{16}O. The release of ^{18}O and ^{16}O from the sample was detected by ion currents for $^{18}O_2$ and $^{16}O^{18}O$ gases in MS. Temperature scan rates for the heating and cooling measurements were 10 °C min^{-1}.

Results and discussion

The sample prepared by high-pressure synthesis was confirmed to be a single phase of fully oxygenated 12R-type hexagonal perovskite $BaFeO_3$, which is considered to consist almost entirely of ^{16}O. The oxygen stoichiometry of the sample was confirmed by the refined full occupancy for the oxygen sites in the SXRD structure analysis. This was also confirmed by the structure analysis using neutron diffraction data, as reported in our previous study.[11] The structure refinement result obtained from the SXRD data for the 12R-type $BaFeO_3$ is given in Fig. S1, and the details of refined structural parameters are also given in Table S1 in the SI. The presence of Fe^{4+} in the sample was also confirmed from the reported Mössbauer spectroscopy results in ref. 11.

Structural stability and reversible oxygen release/incorporation were first remeasured with the present samples. As shown in Fig. S2 of the *ex situ* structure refinements (Fig. S2 and Table S2), the crystal structure returns to its original state upon cooling to room temperature (RT) after heating to 700 °C. *In situ* SXRD patterns collected in air at RT, 700 °C, and RT again (Fig. S3) show that the 12R structure is retained without any signs of decomposition up to 700 °C. Fig. 2 shows the TGA result in an air-like 33% O_2/Ar atmosphere, also confirming the completely reversible loss and uptake of oxygen upon heating the sample to 700 °C. The sample weight begins to decrease at about 400 °C due to oxygen release, eventually reaching 99.3% of the initial weight at 700 °C (corresponding to the oxygen content of 2.89 per formula unit). Note that the sample weight did not change at all in response to holding at 700 °C for 10 min. Upon cooling, the sample weight increases due to oxygen incorporation, as indicated by a cooling curve that traces the initial heating curve. This indicates completely reversible oxygen release and incorporation up to 700 °C, although the previous experiment confirmed the reversibility up to 600 °C.[10] With these results, the optimal annealing temperature for the
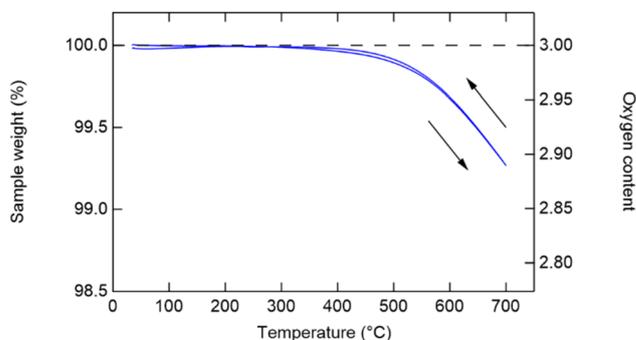

Fig. 2 Sample weight change during TGA of the as-prepared 12R-type $BaFeO_3$ in 33% O_2/Ar between room temperature and 700 °C. The right axis shows the corresponding oxygen content per formula unit.

oxygen isotope exchange is determined to be 650 °C, at which the 12R-type crystal structure remains intact, and the reversible oxygen release/incorporation to the structure is confirmed. Considering that the 150-mg sample is annealed in a 70 mL tube filled with the $^{18}O_2$ gas, which consists of 6.06 mmol ^{18}O and 0.19 mmol ^{16}O, an equilibrium stoichiometry of $BaFe^{18}O_{2.24}^{16}O_{0.76}$ is expected for the isotope exchange experiment.

Fig. 3 shows the TGA/MS results for the 12R-type $BaFeO_3$ sample treated with ^{18}O gas at 650 °C for 2 days. The sample weight decreased significantly above about 460 °C, similar to the previous result,[10] but with a larger weight change. Looking at the data closely, however, it is noted that the sample weight decrease started at about 400 °C in accordance with the development of $^{18}O_2$ and $^{16}O^{18}O$ peaks in the MS. The results confirm that ^{16}O in the initial 12R-type $BaFeO_3$ is exchanged by ^{18}O upon annealing in an $^{18}O_2$ atmosphere and that the exchanged ^{18}O starts to be released from the sample upon heating to temperatures as low as 400 °C. Upon cooling from 700 °C, the sample weight slightly increases and reaches 98.1% of the initial weight of the ^{18}O-exchange-treated 12R-type $BaFeO_3$ at room temperature. This TGA curve on cooling is essentially the same as that obtained for normal 12R-type $BaFeO_3$ (containing only ^{16}O) in air, as shown in Fig. 2. The slight increase in the sample weight upon cooling from 700 °C to about 400 °C is a result of oxygen incorporation from a 33% O_2/Ar atmosphere to return the sample to the $BaFeO_3$ stoichiometry. In other words, the ^{18}O-exchange-treated $BaFeO_3$ releases ^{18}O during heating creating oxygen vacancies and incorporates ^{16}O during cooling to fill those vacancies. Assuming that the sample after the TGA in the air-like atmosphere contains ^{16}O exclusively, the 1.9% weight loss upon cycling gives the initial composition $BaFe^{18}O_{2.3}^{16}O_{0.7}$. This is reasonably consistent with the composition of $BaFe^{18}O_{2.24}^{16}O_{0.76}$ that would be expected if the isotope exchange reached equilibrium conditions.
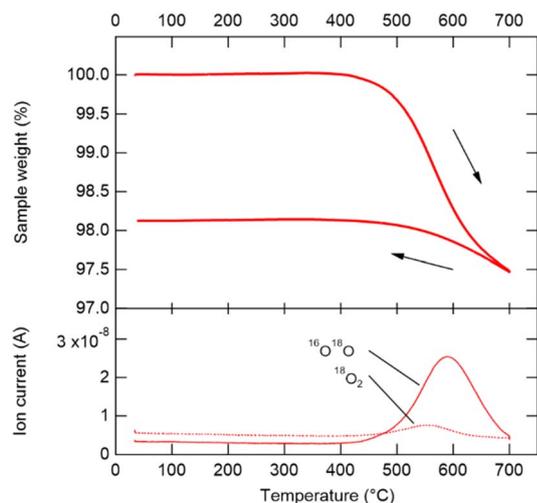
The TGA/MS results, in which the oxygen release from 12R-type $BaFeO_3$ starts at about 400 °C, imply that oxygen in the compound can be mobile at as low as 400 °C. Fig. 4 shows the time-dependent TGA results in a 33% O_2/Ar atmosphere for the sample treated with $^{18}O_2$ gas at 400 °C for 6 days. The data show sample weight changes for 2 cycles between room temperature and 700 °C (RT → 700 °C → RT → 700 °C → RT). The significant decrease in the sample weight during the first heating corresponds to the release of oxygen, which is mainly due to the release of ^{18}O, followed by the increase during cooling due to the incorporation of oxygen (^{16}O). Note that the difference in the sample weights between the initial and final states of the first cycle gives the amount of the ^{18}O isotope in the treated sample, as discussed above. It is also noted that the weight change curves for the second cycle of heating and cooling are exactly the same, indicating that the oxygen (^{16}O) release and incorporation are completely reversible for the heating/cooling cycle to 700 °C. The results confirm that oxygen ions in 12R-type $BaFeO_3$ are undoubtedly exchanged by the ^{18}O isotopes, confirming the significant oxide-ion mobility at temperatures as low as 400 °C. Such low-temperature oxide-ion mobility is presumably facilitated by the unusually high valence state of Fe^{4+}.

Fig. 5 shows the TGA results for samples annealed in ^{18}O gas at 400 °C for 4 and 6 days. Both exhibited weight losses above 400 °C during heating, and the weights did not recover to the initial levels during cooling, confirming the ^{18}O-exchange to ^{16}O in 12R-type $BaFeO_3$. However, the weight loss is larger for the sample treated for 6 days than for the one treated for 4 days. This implies that the ^{18}O isotope exchange rate is determined by kinetics. By annealing the samples in $^{18}O_2$ gas at 400 °C, the amount of ^{16}O exchanged with ^{18}O for 4 days (TGA weight loss of 1.00%) is about half of that for 6 days (weight loss of 1.92%). Apparently, it takes some time for complete isotope exchange to reach an equilibrium state. The results also suggest that the replacement of ^{16}O by ^{18}O occurs through two processes; one involving oxygen loss (and incorporation) and the other involving oxygen exchange while maintaining oxygen stoichiometry. The present result of annealing the sample in $^{18}O_2$ gas
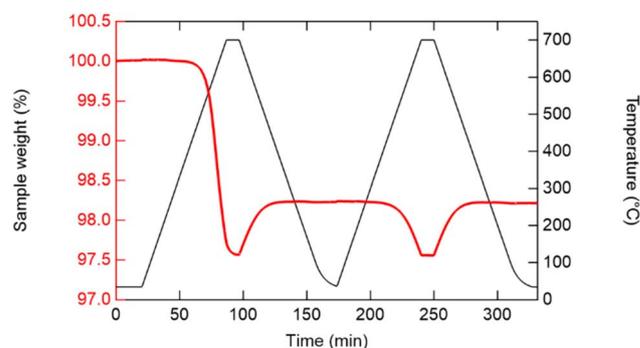

Fig. 3 Sample weight change during TGA of ^{18}O-exchange treated 12R-type $BaFeO_3$ in 33% O_2/Ar, and mass spectrometry of $^{18}O_2$ and $^{16}O^{18}O$ during the heating process.

Fig. 4 Time-dependent sample weight change of 12R-type $BaFe^{18}O_3$ during two cycles of heating/cooling between room temperature and 700 °C. The right axis shows the temperature during the heating/cooling processes.
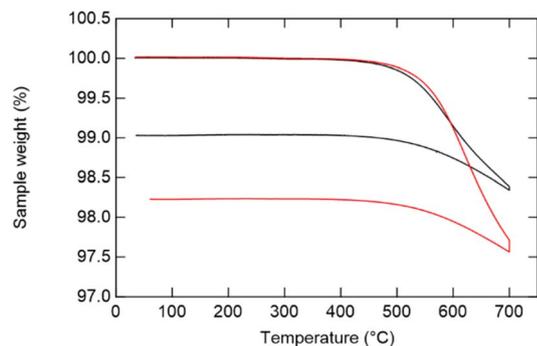
Fig. 5 TGA results for the samples annealed in $^{18}O_2$ gas at 400 °C for 4 (black) and 6 days (red).

at 400 °C implies that the oxygen replacement at this temperature mainly occurs through the exchange process. At a high temperature like 650 °C, however, the oxygen replacement occurs much faster. Therefore, the oxygen replacement is primarily caused by the oxygen release and the oxygen incorporation into the vacant sites. The oxygen exchange process, which maintains stoichiometry, appears to play a minor role in the overall replacement process.

Note again that the ^{18}O isotope exchange rate is determined by kinetics, and annealing for a longer time at a higher temperature can replace more ^{16}O with ^{18}O. The results also suggest that the oxygen exchange is an equilibrium process and is not limited to a specific crystallographic site. The equilibrium stoichiometry of $BaFe^{18}O_{2.24}^{16}O_{0.76}$ obtained by annealing at 650 °C implies that the exchanged ^{18}O ions are located at a 1 : 1 ratio of corner- and face-shared oxygen sites. On the other hand, previous temperature-dependent SXRD results indicated that the oxygen vacancies were preferentially formed at face-shared oxygen sites. The loss of oxygen at the face-shared oxygen sites appears to increase repulsion between the Fe ions facing each other, resulting in an increased Fe–Fe interlayer distance.[10] Although the two conclusions appear to be incompatible, the oxide-ion mobility and the oxygen vacancy stabilization are governed by different mechanisms. The oxide-ion mobility is caused by a series of steps, where oxygen ions hop through many vacant sites. A similar mechanism was discussed in brownmillerite $SrFeO_{2.5}$, where the oxide-ion diffusion is not restricted to the vacancy sites, but other crystallographic sites also participate in chain reactions.[5]

Conclusions

^{18}O-exchange was carried out in the 12R-type hexagonal perovskite $BaFeO_3$ by annealing in an $^{18}O_2$ gas atmosphere. TGA/MS results for the ^{18}O-exchange-treated samples confirm that a large amount of oxygen (^{16}O) in the 12R-type $BaFeO_3$ is replaced by ^{18}O in an equilibrium process. When the ^{18}O-exchange-treated samples are heated in air, ^{18}O is released and ^{16}O is incorporated on cooling, maintaining the 12R-type crystal structure. Thus, completely reversible oxygen release and incorporation up to 700 °C is demonstrated. Oxygen

exchange process with oxygen-ion hopping occurs at temperatures as low as 400 °C, but full exchange in an equilibrium process only occurs over an extended period of annealing, approximately 6 days, implying that the process is governed by kinetics. Although oxide-ion mobility in most oxide materials is believed to occur at higher temperatures, typically 700–800 °C as seen in solid-oxide fuel cell materials, the present results clearly demonstrate that oxide-ion hopping can occur at temperatures as low as 400 °C in oxides such as $BaFeO_3$ containing unusually high valence Fe^{4+}. The results provide new insights into the fundamental oxide-ion mobility in materials of interest for energy-related applications.

Author contributions

R. W., W. P., and Y. S. conceived the idea and initiated the project. R. W. and M. G. prepared the samples, and R. W., W. P., and Y. S. performed the thermogravimetric and structural analysis. W. P. and Y. S. supervised the project. All authors discussed the experimental results and wrote the manuscript.

Conflicts of interest

There are no conflicts to declare.

Data availability

The data supporting this article have been included as part of the supplementary information (SI), Supplementary information: which consists of results of (1) Rietveld refinement for the 12R-type $BaFeO_3$ synthesized under a high-pressure condition, (2) Rietveld refinement for the 12R-type $BaFeO_3$ at room temperature after heating at 700 °C, and (3) *in situ* SXRD for the 12R-type $BaFeO_3$ in air at room temperature, 700 °C, and room temperature again. See DOI: https://doi.org/10.1039/d5ta09711h.

Acknowledgements

References

1 B. C. H. Steele and A. Heinzel, *Nature*, 2001, **414**, 345–352.

2 J. B. Goodenough, *Annu. Rev. Mater. Res.*, 2003, **33**, 91–128.

3 M. High, C. F. Patzschke, L. Zheng, D. Zeng, O. Gavalda-Diaz, N. Ding, K. H. H. Chien, Z. Zhang, G. E. Wilson, A. V. Berenov, S. J. Skinner, K. L. Sedransk Campbell, R. Xiao, P. S. Fennell and Q. Song, *Nat. Commun.*, 2022, **13**, 5109.

4 A. Trovarelli, *Comments Inorg. Chem.*, 1999, **20**, 263–284.

5 W. Paulus, H. Schober, S. Eibl, M. Johnson, T. Berthier, O. Hernandez, M. Ceretti, M. Plazanet, K. Conder and C. Lamberti, *J. Am. Chem. Soc.*, 2008, **130**, 16080–16085.

6 T. Motohashi, T. Ueda, Y. Masubuchi, M. Takiguchi, T. Setoyama, K. Oshima and S. Kikkawa, *Chem. Mater.*, 2010, **22**, 3192–3196.

7 K. Beppu, S. Hosokawa, K. Teramura and T. Tanaka, *J. Mater. Chem. A*, 2015, **3**, 13540–13545.

8 H. Guo, M. Amano Patino, N. Ichikawa, T. Saito, R. Watanabe, M. Goto, M. Yang, D. Kan and Y. Shimakawa, *Chem. Mater.*, 2022, **34**, 345–350.

9 Y. Shimakawa, M. Goto and M. Amano Patino, *ECS J. Solid State Sci. Technol.*, 2022, **11**, 043004.

10 R. Watanabe, M. Goto, Y. Kosugi, D. Kan and Y. Shimakawa, *Chem. Mater.*, 2024, **36**, 2106–2112.

11 Z. Tan, F. D. Romero, T. Saito, M. Goto, M. Amano Patino, A. Koedtruad, Y. Kosugi, W.-T. Chen, Y.-C. Chuang, H.-S. Sheu, J. P. Attfield and Y. Shimakawa, *Phys. Rev. B*, 2020, **102**, 054404.

12 S. Corallini, M. Ceretti, G. Silly, A. Piovano, S. Singh, J. Stern, C. Ritter, J. Ren, H. Eckert, K. Conder, W. Paulus, W.-t. Chen, F.-C. Chou, N. Ichikawa and Y. Shimakawa, *J. Phys. Chem. C*, 2015, **119**, 11447–11458.

13 S. Corallini, M. Ceretti, A. Cousson, C. Ritter, M. Longhin, P. Papet and W. Paulus, *Inorg. Chem.*, 2017, **56**, 2977–2984.

14 S. Hu, Y. Du, J. Li, C. Liu, H. Fu, J. Qin, H. Zhang and B. Chen, *Phys. Chem. Chem. Phys.*, 2023, **25**, 25492–25512.

15 Y. Li, M. Chen, L. Jiang, D. Tian and K. Li, *Phys. Chem. Chem. Phys.*, 2024, **26**, 1516–1540.

16 F. Izumi and K. Momma, *Solid State Phenom.*, 2007, **130**, 15–20.

17 K. Momma and F. Izumi, *J. Appl. Crystallogr.*, 2011, **44**, 1272–1276.